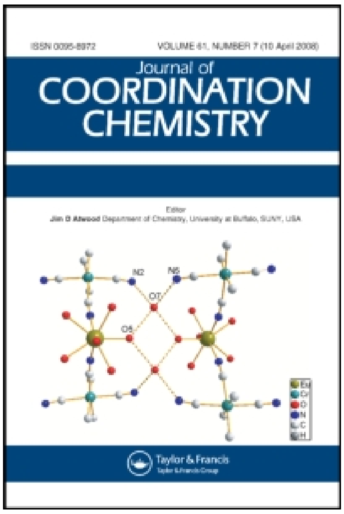

Journal of Coordination Chemistry
Publication details, including instructions for authors and subscription information:
http://www.informaworld.com/smpp/title~content=t713455674

An 18-member dinucleating unsymmetrical [N_{10}] macrocycle and its bimetallic complexes $M_2LCl_2(ClO_4)$ (M=Co, Ni, Cu, Zn, Cd or Hg)

Z. A. Siddiqi[a]; R. Arif[a]; S. Kumar[a]; Md. Khalid[a]
[a] Division of Inorganic Chemistry, Department of Chemistry, Aligarh Muslim University, Aligarh 202002, India

To cite this Article Siddiqi, Z. A. , Arif, R. , Kumar, S. and Khalid, Md.(2008) 'An 18-member dinucleating unsymmetrical [N_{10}] macrocycle and its bimetallic complexes $M_2LCl_2(ClO_4)$ (M=Co, Ni, Cu, Zn, Cd or Hg)', Journal of Coordination Chemistry, 61: 13, 2032 — 2045

To link to this Article: DOI: 10.1080/00958970701824332

URL: http://dx.doi.org/10.1080/00958970701824332

Journal of Coordination Chemistry
Vol. 61, No. 13, 10 July 2008, 2032–2045

An 18-member dinucleating unsymmetrical [N_{10}] macrocycle and its bimetallic complexes $M_2LCl_2(ClO_4)$ (M = Co, Ni, Cu, Zn, Cd or Hg)

Z. A. SIDDIQI*, R. ARIF, S. KUMAR and MD. KHALID

Division of Inorganic Chemistry, Department of Chemistry,
Aligarh Muslim University, Aligarh 202002, India

(*Received 24 April 2007; in final form 6 June 2007*)

The 18-member unsymmetrical dinucleating Shiff-base decaaza [N_{10}] macrocyclic ligand, 2,8,11,17-tetramethyl-3,5,7,12,14,16-hexaphenyl-[1,3,5,7,9,10,12,14,16,18] decaazaoctadeca-2,8,11,17-tetraene dihydroperchlorate ($L \cdot 2HClO_4$) was obtained as a cream colored solid from reaction of N-acetylaniline and hydrazine in the presence of $HClO_4$ followed by cyclization (capping) using aniline and excess HCHO in methanol at RT. Reactions of $L \cdot 2HClO_4$ with MCl_2 and $[M(Ph_3P)_2Cl_2]$ afforded air stable complexes, $M_2LCl_4(ClO_4)_2$ (M = Co, Ni, Cu, Zn or Cd). The compounds have been characterized by physico-chemical and spectroscopic studies. FAB–Mass spectral data support bimetallic coordination by the macrocycle. IR studies confirm coordination/encapsulation of metal ions involving unsymmetrical aza sites. Magnetic susceptibility and UV–Visible data indicate a low-spin, five-coordinate geometry for Co(II) and Ni(II) complexes. The anisotropic EPR signals ($g_{\parallel} > g_{\perp}$) for Cu^{2+} complex suggest an axial type tetragonality. Molecular model computations have been employed for a theoretical perspective of the ligand and complexes. The important bond lengths and bond angles have been estimated using CS Chem-3D software. The ionic association constant (K_1) and thermodynamic free energy change (ΔG) were evaluated from the conductometric data of the complexes, which indicate presence of a strong ion-pair even in solution. Cyclic voltametric studies on solutions of $M_2LCl_4(ClO_4)_2$ (M = Co, Ni or Cu) in DMSO indicate reversible and quasi-reversible redox couples.

Keywords: Unsymmetrical [N_{10}] macrocycle; Dinucleating macrocycle; Homo–bimetallic complexes; Molecular model; Cyclic voltametric studies

1. Introduction

Polynucleating macrocyclic ligands, which bind two or more metal ions, have received attention [1–4], with important implications for a range of chemical and biochemical applications. Many metallo-proteins [5, 6] and a variety of metallo-enzymes [5–8] have polymetallic centers with electron rich coordination sites. Metal complexes of some dinucleating hexaaza macrocycles form host-guest complexes with a range of anions such as maleate, pyrophosphate, triphosphate, etc. [9]. Polymetallic complexes often display interesting catalytic activities especially in hydrolysis of peptidase [10] and

---

*Corresponding author. Email: zafarasiddiqi@yahoo.co.in

Journal of Coordination Chemistry
ISSN 0095-8972 print/ISSN 1029-0389 online © 2008 Taylor & Francis
DOI: 10.1080/00958970701824332

phosphate derivatives [11]. Study of such polynuclear macrocyclic complexes help understanding the mutual influences [12] of the two neighboring metal centers on electronic, magnetic and electrochemical properties. The asymmetric nature of some homo-bimetallic as well as hetero-bimetallic transition metal derived metallo–biosites, where the individual metal ions exhibit different roles in the function of the metallo-enzyme, has led to carefully designed unsymmetrical [13–15] polynucleating macrocycles. Macrocyclic ligands with dissimilar coordination sites are classified as unsymmetrical macrocyles. Complexes of such macrocycles are thermodynamically stable and kinetically retarded with regard to metal ion dissociation [16]. Large dinucleating polyaza macrocycles $[N_k]$ (where $k > 6$) are prepared [2, 3, 16] with step-wise cyclization reactions. Most early efforts [8] describe metal complexes of symmetrical polyaza macrocycles. Preparation of such complexes usually involve template procedure using metal ions as templating agents [6, 16]. However, compatibility between size of the templating ions and the hole (cavity) size of the macrocycles is a key factor, responsible for the effectiveness [16] of this procedure. The preparation of metal ion free polyaza $[N_k]$ macrocycles having unsymmetrical coordination environments i.e. with iminic and aminic binding sites have been reported [2, 17] where $k \leq 8$. However, unsymmetrical polyaza macrocycles with $k > 8$ to encapsulate more than one metal ion are not common [3, 17]. We have, recently, reported [3] 20-membered $[N_8]$ and 32-membered $[N_{12}]$ unsymmetrical macrocycles capable to encapsulate two metal ions in the macrocyclic cavities. A versatile synthetic route to prepare unsymmetrical dinucleating macrocyles uses an in-situ generation of a reactive intermediate containing (–C=N–) bonds. Herein we report the synthetic viability of this reactive intermediate for isolation of a 18-membered unsymmetrical decaaza $[N_{10}]$ macrocycle, 2,8,11,17-tetramethyl-3,5,7,12,14,16-hexaphenyl [1,3,5,7,9,10,12,14,16,18] decaazaocta deca-2,8,11,17-tetraene dihydroperchlorate. The ligand produces homo-bimetallic complexes with Co^{2+}, Ni^{2+}, Cu^{2+}, Zn^{2+}, Cd^{2+} and Hg^{2+}, which have been characterized using spectroscopic and electrochemical techniques.

2. Experimental

All reagents were commercially pure and used as received except metal salts, which were recrystallized and dried over P_4O_{10} in a desiccator. The precursors $[M(Ph_3P)_2Cl_2]$ ($M = Co$, Ni, Zn, Cd or Hg) were prepared by reported methods [3, 18]. Solvents were purified before used.

2.1. *Preparation of 2,8,11,17-tetramethyl-3,5,7,12,14,16-hexaphenyl [1,3,5,7,9,10,12,14,16,18]decaazaoctadeca-2,8,11, 17-tetraenedihydro-perchlorate i.e.* $[L \cdot 2HClO_4]$

N-acetylaniline (30.6 g, 0.2 mol) was slowly dropped into a mixture containing hydrazine hydrate (6.05 mL, 0.1 mol) and $HClO_4$ (10 mL, 0.1 mol) in 30 mL methanol with continuous stirring at room temperature. The reaction mixture was then stirred for 2 days and the progress of the reaction monitored by UV–Visible spectra. The intensity of the 320 nm band characteristic of $n \rightarrow \pi^*$ transition of the *N*-acetylaniline diminishes with concomitant appearance of an absorption band at 385 nm band indicative of formation of the intermediate. An excess of HCHO (41 mL, 0.3 mol) and aniline (9.0 mL, 0.1 mol) were dropped at a slow rate with vigorous stirring at room temperature. The reaction is exothermic and produces cream colored suspension. The reaction mixture was vigorously stirred overnight. The cream colored precipitate was filtered off, washed first with methanol and finally by dry ether. It was then dried over P_4O_{10} in a desiccator (yield 27.8 g ~ 30%, m.p. 128–130°C). The product was recrystallized from dioxane giving microcrystalline solid, which melts sharply at 130°C. Anal. Calcd for $C_{48}H_{52}N_{10}Cl_2O_8$ (%): C, 59.62; H, 5.17; N, 14.49; Found: C, 59.61; H, 5.16; N, 14.48.

2.2. *Preparation of $M_2LCl_2(ClO_4)_2$ [M = Co(1), Ni(2), Cu(3), Zn(4), Cd(5) or Hg(6)]*

A methanolic solution of $CoCl_2 \cdot 6H_2O$ (0.50 g, 2.0 mmol), $NiCl_2 \cdot 6H_2O$ (0.50 g, 2.0 mmol), $CuCl_2 \cdot 2H_2O$ (0.34 g, 2.0 mmol), $ZnCl_2$ (0.28 g, 2.0 mmol), $CdCl_2 \cdot 5H_2O$ (0.45 g, 2.0 mmol) or $HgCl_2$ (0.55 g, 2.0 mmol) was added drop-wise to the ligand (1.0 g, 1.0 mmol) in 30 mL dioxane with stirring at RT. The reaction mixture was stirred for 12h. The precipitate that formed was filtered off, washed with dioxane followed by methanol and then dried under vacuum. [**1** green color, m.p. 280°C dec., **2** yellow-brown, m.p. 278°C dec., **3** brownish-green, m.p. 270°C dec., **4** off-white, m.p. 282°C dec., **5** light-yellow, m.p. 288°C dec., **6** light-grey, m.p. 310°C dec.]. Anal. Calcd for $C_{48}H_{50}N_{10}Cl_4O_8Co_2$: C, 49.91; H, 4.33; N, 12.13; Co, 10.21; Cl, 12.30. Found for **1**: C, 49.90; H, 4.31; N, 12.10; Co, 10.20; Cl, 12.20. Anal. Calcd for $C_{48}H_{50}N_{10}Cl_4O_8Ni_2$: C, 49.94; H, 4.33; N, 12.13; Ni, 10.17; Cl, 12.31. Found for **2**: C, 49.93; H, 4.31; N, 12.10; Ni, 10.15; Cl, 12.20. Anal. Calcd for $C_{48}H_{50}N_{10}Cl_4O_8Cu_2$: C, 49.50; H, 4.20; N, 12.03; Cu, 10.92; Cl, 12.20. Found for **3**:C, 49.50; H, 4.19; N, 12.01; Cu, 10.90; Cl, 10.19. Anal. Calcd for $C_{48}H_{50}N_{10}Cl_4O_8Zn_2$: C, 49.36; H, 4.28; N, 11.99; Zn, 11.20; Cl, 12.17. Found for **4**: C, 49.35; H, 4.28; N, 11.90; Zn, 11.10; Cl, 12.00. Anal. Calcd for $C_{48}H_{50}N_{10}Cl_4O_8Cd_2$: C, 45.71; H, 3.90; N, 11.10; Cd, 17.83; Cl, 11.20. Found for **5**:C, 45.69; H, 3.80; N, 11.00; Cd, 17.50; Cl, 11.00. Anal. Calcd for $C_{48}H_{50}N_{10}Cl_4O_8Hg_2$: C, 40.07; H, 3.47; N, 9.74; Hg, 27.90; Cl, 9.88. Found for **6**: C, 40.06; H, 3.40; N, 9.80; Hg, 27.80; Cl, 9.50.

The reactions of $L \cdot 2HClO_4$ with $[M(Ph_3P)_2Cl_2]$ (M = Co, Ni, Zn, Cd or Hg) also resulted in complexes **1**, **2**, **4**–**6** in quantitative yields as following: A methanolic solution of $[Co(Ph_3P)_2Cl_2]$ (0.65 g, 1.0 mmol), $[Ni(Ph_3P)_2Cl_2]$ (0.65 g, 1.0 mmol), $[Zn(Ph_3P)_2Cl_2]$ (0.68 g, 1.0 mmol), $[Cd(Ph_3P)_2Cl_2]$ (0.55 g, 1.0 mmol) or $[Hg(Ph_3P)_2Cl_2]$ (0.55 g, 1.0 mmol) was reacted with $L \cdot 2HClO_4$ (0.5 g, 1.0 mmol) solution in 20 mL dioxane with stirring at RT. The solid product formed was filtered, washed with dioxane followed by methanol and then dried under vacuum as above. The physical appearance, melting point, analytical data as well as spectral features of the final products were identical to the corresponding complexes **1**–**6** described above. The filtrate and washing in each case were evaporated to dryness then extracted in acetone, which was kept at 5°C for ~72h. This gave colorless needles (m.p. 80°C), identified as triphenylphosphine from analytical, IR and NMR spectroscopic data.

2.3. *Physical measurements*

IR spectra were recorded as KBr discs on a Perkin-Elmer Model spectrum GX spectrophotometer. ^{1}H- and ^{13}C-NMR spectra (deuterated DMSO) were recorded on a Brucker DRC-300 spectrometer using $SiMe_4$ (TMS) as internal standard. Solvent indicated a strong signal at $2.5\,\delta$ for ^{1}H- and $39.8\,\delta$ for ^{13}C- with reference to TMS. Electronic spectra and conductivities of 10^{-3} M solutions in DMSO were recorded on a Cintra-5GBS UV−Visible spectrophotometer and Systronics-305 digital conductivity bridge, respectively, at room temperature. FAB–Mass spectra were recorded on Jeol-SX102 spectrometer using argon as the FAB gas. The accelerating voltage was 10KV and spectra were recorded in m-nitrobenzyl alcohol (NBA) matrix. The matrix peaks appear at $m/z = 136$, 137, 154, 289 and 307. The X-band EPR spectra of polycrystalline samples were recorded on a Jeol-RE series Model JES-RE3X spectrometer at RT and −196°C calibrated with diphenylpicrylhydrazy (dpph: $g = 2.003$). Magnetic susceptibilities were estimated at room temperature using a Faraday balance calibrated with $Hg[Co(NCS)_4]$. Microanalysis was obtained from the Micro-Analytical Laboratory of CDR Institute, Lucknow, India. Cyclic voltamograms were recorded on a CH-Instrument Electro-Chemical Analyzer using tetraethylammonium perchlorate as a supporting electrolyte at room temperature. A three cell electrode is used which contains a Pt micro cylinder working electrode, Pt wire as auxillary electrode and Ag/AgCl as the reference electrode.

3. Results and discussion

Reaction of hydrazine with *N*-acetylaniline in 1 : 2 mol ratio in the presence of perchloric acid at RT (first step) generates an intermediate, *N*,*N*′-*bis*(*N*-ethylaniline)-hydrazine-1,2-diimine, which contains two iminic (C=N) bonds. Formation of the intermediate during the condensation was monitored by the electronic spectrum of the reaction mixture. The disappearance of the absorption at 320 nm characteristic [2, 3] of the $n \rightarrow \pi^*$ transition of (–CO–NH–) group of *N*-acetylaniline with the concomitant appearance of a new band at 385 nm characteristic of the $\pi \rightarrow \pi^*$ transition [3, 19] of iminic (C=N) bond, is indicative of the completion of reaction. The in-situ capping reaction (secondary step) of this reactive substrate with excess HCHO (3 mole equivalent) and aniline (1 mole equivalent) induced the 2 + 2 cyclization (figure 1) affording a cream stable solid. The presence of $HClO_4$ in the reaction mixture not only [2, 20] facilitates the capping (cyclization) reactions but also helps in the isolation of the dihydro perchlorate salts $[L \cdot 2H][ClO_4]_2$ of the macrocyclic ligand. Preparation of metal ion free macrocycles usually require the presence of mineral acids (HCl, HNO_3 or $HClO_4$) which minimize the extent [2, 3, 20] of unwanted side reactions such as polymerization. The probable mechanism for the synthesis is displayed in figure 1. Analytical and FAB–Mass spectral data are consistent with the molecular formula $C_{48}H_{52}N_{10}Cl_2O_8$ or $L \cdot 2HClO_4$, with a prominent peak (~62% abundance) at $m/z = 766$ assignable to the molecular ion peak $[L]^+$ along with various important fragmentation products, viz $1/2[L]^+$ ($m/z = 383$), $[(PhNHCH)_2]^+$ ($m/z = 212$), $[(Ph)_2]^+$ ($m/z = 254$), $[PhNHCH_2N]^+$ ($m/z = 120$) and $[PhCH_2]^+$ ($m/z = 106$) etc., (table 1), which are in good agreement with the proposed structure (figure 1) of the macrocyclic moiety.

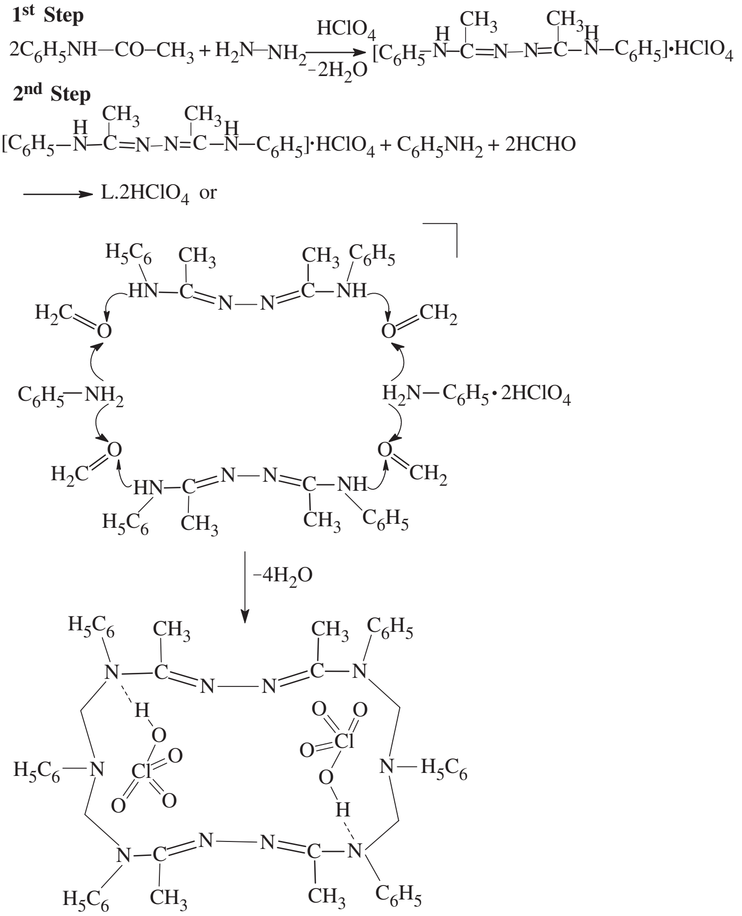

Figure 1. Mechanism of the formation of dinucleating macrocyclic ligand, L · $2HClO_4$.

Table 1. Important peaks positions (*m*/*z*) with their assignments for FAB-mass spectra of L · $2HClO_4$ and **1**–**3**.

	Species
L · $2HClO_4$	$[L]^+$ ($m/z = 766$); 1/2$[L + H]^+$ ($m/z = 384$); $[L + Rn]^+$ ($m/z = 1055$); $[(PhNHCH_2)_2 + H]^+$ ($m/z = 213$); $[(Ph)_2]^+$ or NBA^+ ($m/z = 154$); $[PhNHCH_2N]^+$ ($m/z = 120$); $[PhNHCH_2]^+$ ($m/z = 106$).
1	$[Co_2(L)Cl_2(ClO_4)_2 + H]^+$ ($m/z = 1149$); $[Co_2(L)Cl_2(ClO_4) + H]^+$ ($m/z = 1059$); $[Co_2(L)Cl_2]^+$ ($m/z = 950$); $[Co_2(L) + H]^+$ ($m/z = 881$)
2	$[Ni_2(L)Cl_2(ClO_4)_2 + H]^+$ ($m/z = 1159$); $[Ni_2(L)Cl_2(ClO_4) + H]^+$ ($m/z = 1052$); $[Ni_2(L)Cl_2]^+$ ($m/z = 952$); $[Ni_2(L) + H]^+$ ($m/z = 883$)
3	$[Cu_2(L)Cl_2(ClO_4)_2 + H]^+$ ($m/z = 1161$); $[Cu_2(L)Cl_2(ClO_4) + H]^+$ ($m/z = 1062$); $[Cu_2(L)Cl_2]^+$ ($m/z = 962$); $[Cu_2(L) + H]^+$ ($m/z = 893$)

NBA (*m*-nitrobenzyl alcohol) was used as the matrix for FAB recording which give peaks at [$m/z = 136$, 137, 154, 289, 307]. Bq = NBA (136); Rn = NBA (289).

Table 2. Important frequencies (cm^{-1}) in IR spectra of L · 2HClO$_4$ and complexes with their assignments.

					ClO_4			
Comp.	ν(N–N)	ν(C=N)	Aliphatic ν(C–N)	Aromatic ν(C–N)	ν_1	ν_2	ν_3	ν(M–N)
L · 2HClO$_4$	987s	1613vs	1245s	1348s	1172m	1075s 1118s	620w	–
1	982m	1600s	1260m	1355s	1175s	1042m 1026m	620w	416, 428
2	986m	1595s	1248s	1353s	1172s	1043w 1031m	622w	418, 440
3	985mb	1592s	1262s	1343s	1170m	1062w 1044m	612w	426, 438
4	950m	1603s	1248m	1334m	1172m	1074m 1062m	618w	425, 475
5	952m	1600s	1256m	1345s	1174m	1104w 1098m	622w	416, 448
6	964m	1598s	1258m	1351s	1175m	1095w 1078m	624w	422, 456

m = Medium, mb = Medium broad, s = strong, w = weak.

^{1}H–NMR spectrum recorded in d$_6$-DMSO does not show any signal attributable to NH protons supporting the condensation process. The spectrum exhibits a multiplet for C_6H_5 protons (6.7 δ, $J_{HH} = 5$) and two singlets for CH_3 protons (2.0 δ) and methylene, –CH$_2$– protons (3.2 δ). ^{13}C-NMR spectrum of the ligand exhibits a resonance in 113–143 δ characteristic [2] of C=C bonds. Additional signals at 70.5 δ and 9.4 δ are due to C=N and CH_3 carbons, respectively. The UV-Visible spectrum of L · 2HClO$_4$ in DMSO shows a strong absorption band at 385 nm (€ $= 1.5 \times 10^3$ Lmole^{-1} cm^{-1}) due to $\pi \rightarrow \pi^*$ transition of the iminic (C=N) bond [3, 19]. The frequencies observed in the IR spectrum (table 2) of the macrocyclic ligand are assignable to ν(N–N), ν(C=N), ν(C–N), ν(C=C), ν(C–N), ν(C–C) and ν(C–H) fundamental stretching vibrations [3, 21] as well as the fundamental frequencies of perchlorate counter ion (ν_1, ν_2, ν_3) [22]. The spectrum does not show absorption in the 1700–1750 cm^{-1} region characteristic of ν(C=O) stretching vibration of the (–CO–NH–) linkage supporting the proposed mechanism (figure 1). The observed splitting of ν_2 stretching vibration of ClO_4 ion in the region 1000–1150 cm^{-1} (table 2) indicates lowering in symmetry [22] relative to T_d symmetry of the free perchlorate anion. The magnitude of molar conductance ($\Lambda_m = 17.0$ ohm mol^{-1} cm^2) measured in DMSO (dielectric constant = 46) indicates a non-electrolytic nature [23] of the macrocyclic salt L · 2HClO$_4$. This non-ionic behavior in solution suggests that the salt does not dissociate due to strong cation–anion interaction between the macrocyclic cation [L · 2H]$^{2+}$ and the [ClO$_4$]$^-$ counter anion. Protonated large polyaza [N$_8$] and [N$_{10}$] macrocycles are reported [3, 24] to encapsulate the counter anions e.g. succinate, NO_3^-, ClO_4^- or even complex anions. The physico-chemical and spectroscopic studies agree with formation of an 18-member unsymmetrical [N$_{10}$] macrocycle consisting of iminic (C=N) and aminic (C–N–C) functions [2, 23] in 2,8,11,17-tetramethyl-3,5,7,12,14,16-hexaphenyl [1,3,5,7,9,10,12,14,16,18] decaazaoctadeca-2,8,11,17-tetraene dihydroperchlorate i.e. L · 2HClO$_4$.

Reactions of the macrocyclic ligand with metal chlorides, MCl$_2$ (M = Co, Ni, Cu, Zn, Cd or Hg) result in products whose analytical data (Experimental section) indicate

[$M_2C_{48}H_{50}N_{10}Cl_4O_8$] [M = Co(**1**), Ni(**2**), Cu(**3**), Zn(**4**), Cd(**5**) or Hg(**6**)] consistent with $M_2LCl_2(ClO_4)_2$ homo-bimetallic complexes. The reactions of $L \cdot 2HClO_4$ with [$M(Ph_3P)_2Cl_2$] are accompanied with total liberation of PPh_3 affording final products whose colors, melting points as well as analytical data are identical to **1**–**6**. This preferential chelation of metal ions by $L \cdot 2HClO_4$ is apparently, the consequence of the well known macrocyclic effect.

The FAB–Mass spectra of **1**–**3** contain envelopes of peaks with the most intense expected isotopic bands whose *m*/*z* values = 1149, 1159 and 1161 are consistent with the molecular ion $[Co_2LCl_2(ClO_4) + H]^+$, $[Ni_2LCl_2(ClO_4) + H]^+$ and $[Cu_2LCl_2(ClO_4) + H]^+$, respectively (table 1). These species lose the exocyclic ligands through step-wise fragmentations to give $[Co_2L + H]^+$, $[Ni_2L + H]^+$ and $[Cu_2L + H]^+$ species, respectively. The *m*/*z* values of significant fragments in the spectra with their assignments are summarized in table 1. Peaks due to the fragmentations of the endocyclic substitutents of the ligand (vide supra) as well as of the matrix were also present in the spectra of the complexes. The envelope of bands consistent with the expected isotopic peaks is a characteristic feature for bimetallic species. The FAB–Mass data therefore, strongly support that **1**–**3** retain bimetallic coordination with the macrocycle even under FAB–Mass spectral conditions.

The molar conductivities of 10^{-3} M solution of **1**–**3** in DMSO, $\Lambda_m \approx 50\,\text{ohm}\,\text{mol}^{-1}\,\text{cm}^2$, are comparable to a 1 : 1 electrolyte [23] in solution. However, complexes **4**–**6** were not soluble in organic solvents indicating an ologomeric nature. IR spectra of all complexes show characteristic absorption frequencies due to ν(N–N), ν(C=N), ν(C–N) and perchlorate (ν_1,ν_2,ν_3) stretching vibrations (table 2). A small shift in the position of ν(N–N) and ν(C=N) stretching vibrations relative to the free ligand has been observed after complexation. The (M–N) bond stretching vibration has been observed as a medium intensity doublet in 400–500 cm^{-1} region confirming [3, 21] encapsulation of the metal ions through aza groups in the macrocyclic cavity. Chelation of metal ions through unsymmetrical aza coordination sites of the iminic and aminic functions in the macrocycle is probably responsible for the observed splitting of the ν(M–N) stretching vibration.

3.1. *Magnetic susceptibility, EPR spectroscopic and electronic ligand field spectral studies*

The μ_{eff} value of **1** is 2.45 B.M. (or μ_{eff} per $Co^{2+} = 1.23$ B.M.), which is significantly lower than the theoretical spin-only value (μ_{so} per $Co^{2+} = 3.87$ B.M.) for three unpaired electrons on each Co^{2+} ion [25] in a homo-bimetallic complex with two magnetically non-interacting spins $[(S^{2+}_{Co} - S^{2+}_{Co}) = (3/2, 3/2)]$ in the absence of any exchange interaction [26]. The observed magnetic moment for **3** is 2.25 B.M. (or μ_{eff} per $Cu^{2+} = 1.13$ B.M.). Here too, the observed magnitude is lower than that of 2.83 B.M., expected for a homo-bimetallic Cu(II) complex containing two un–coupled spins $[(S^{2+}_{Cu} - S^{2+}_{Cu}) = (1/2, 1/2)]$. These results indicate that the binuclear units are not magnetically isolated. The presence of antiferromagnetic exchange lowers the magnetic moments. This is not an unusual phenomenon, because intramolecular antiferromagnetic interaction [27] exists in many binuclear complexes. The room temperature EPR spectrum of powdered samples of **3** is anisotropic and exhibits two signals with g_ψ and g_ζ at 2.21 and 2.05, respectively. This behavior is reported [28] to be characteristic of

Table 3. μ_{eff} (B.M.) and electronic spectral data of the complexes with their assignments.

Complexes	μ_{eff} (B.M.)	Band positions ν (nm)	 ν (cm^{-1})	 Band assignments	Extinction ε^a	Coefficient ε/atom
1	2.45	385	25,974	$\pi^* \leftarrow \pi + CT$	1752	87
		482	20,746	$b_1 \leftarrow a_1$	235	117
		571	17,513	$a_1 \leftarrow e$	139	69
		685	14,598		498	250
2	Diamagnetic	395	25,316	$\pi^* \leftarrow \pi + CT$	1823	911
		506	19,762	$^1E' \leftarrow ^1A'_1$	236	118
		562	17,793	$^1E'' \leftarrow ^1A_1$	230	115
		571	17,543		265	132
3	2.25	380	26,315	$\pi^* \leftarrow \pi + CT$	1752	876
		570	15,384	$^2A_{2g} \leftarrow ^2E_g$	988	494

[a] Molar extinction coefficient (lit mol^{-1} cm^{-1}).

homo–bimetallic Cu(II) where $g_\psi > g_\zeta > 2.0$ is typical of axially symmetric (d^9) Cu^{2+} ion having the unpaired spins $[(S^{2+}_{Cu} - S^{2+}_{Cu}) = (1/2, 1/2)]$ in a $d_{x^2-y^2}$ orbital [29]. The electronic spectrum shows a broad absorption band centered at 650 nm (or 15384 cm^{-1}) assigned to $^2T_2g \leftarrow ^2Eg$ transition for an octahedral environment around Cu^{2+} ion [30].

Complex **2** is diamagnetic and exhibits ligand field (d–d) bands in 506–670 nm (19762–17543 cm^{-1}) region, attributed to low-spin d^8 having a trigonal–bipyramidal geometry [30]. The ground state configuration of Ni^{2+} in diamagnetic trigonal–bipyramidal geometry is $^1A'_1$ and the excited states are $^1E'$ and $^1E''$ giving two spin-allowed transitions $^1E' \leftarrow ^1A'_1$ and $^1E'' \leftarrow ^1A'_1$. The positions of the absorption bands with their assignments are shown in table 3. The doublet observed at 17,000–18,000 cm^{-1} is a split component of the $^1E'' \leftarrow ^1A'_1$ transition, probably due to symmetry lowering of the basal coordination plane resulting in distorted coordination around Ni^{2+}.

Complexes **1**–**3** show a strong band at 380–395 nm (26,345–25,974 cm^{-1}), assigned to $L \rightarrow M$ charge transfer as well as to $\pi \rightarrow \pi^*$ transition associated with azomethine (C=N) group [3, 17]. The ligand field for **1** is comparable to that reported [30–32] for low–spin mononuclear Co^{2+} complexes having a distorted five-coordinate geometry. The magnetic moment values for such complexes are [33] in the 2.5–3.0 BM range. The observed ligand field bands with their assignments are given in table 3. Five-coordinate mononuclear Co^{2+} complexes of the type $[CoL_2X]$ [L = diphenyl(o-diphenyl arsinophenyl)phosphine] are reported [33] to exhibit $\mu_{eff} \cong 2.5$ BM. The considerable decrease in the μ_{eff} value therefore, suggests the presence of an antiferromagnetic magnetic coupling between the neighboring metal ions.

3.2. *Molecular model studies*

We have employed molecular modeling based on the CS Chem–3D programme, to provide energy plots for the best structure of the ligand and the complexes. The structure of the ligand (figure 2a) indicates that the aza coordinating sites (including iminic and aminic function) in the macrocyclic ligand are not well oriented to

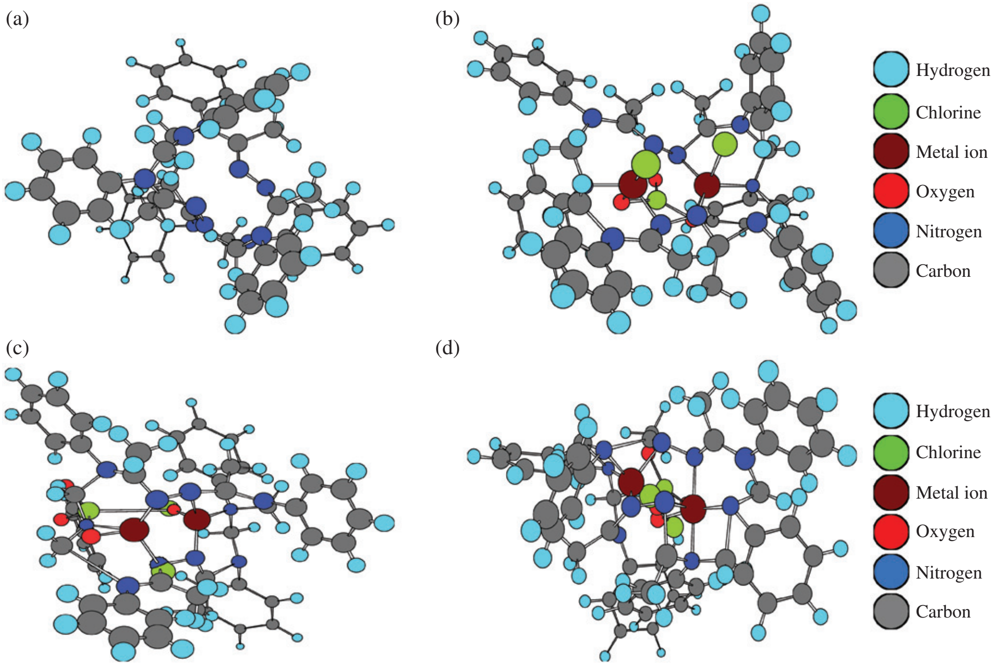

Figure 2. (a) Computed structural perspective of the ligand, $L \cdot 2HClO_4$. (b) Computed coordination geometry around Co^{2+} ion in **1**. (c) Computed coordination geometry around Ni^{2+} ion in **2**. (d) Computed coordination geometry around Cu^{2+} ion in **3**.

provide a perfect tridentate [N,N,N] or tetradentate [N,N,N,N] basal plane. However, encapsulation/chelation of metal ions Co^{2+}, Ni^{2+} (figure 2b, 2c) and Cu^{2+} (figure 2d) appear to be effective in bringing the chelating aza sites [N,N,N] and [N,N,N,N] per metal ions, respectively, into the basal planes of the macrocyclic cavities. The tridentate chelation for Co^{2+}or Ni^{2+} results in a five-coordinate trigonal-bipyramidal geometry in the homo–bimetallic **1** and **2**. For **3** a six-coordinate distorted octahedral geometry exists. The semi-empirical CS–MOPAC computation [34, 35] has been used to measure bond lengths and angles for the optimum structural plots of the ligand as well as the metal complexes. The important computed bond lengths as well as bond angles are summarized in table 4. The computed (M–N) bond distance (table 4) in the present complexes is shorter than that reported (c.f. ~1.96 A°) [36] for the polyaza macrocyclic complexes involving non-functionalized aminic aza coordinating sites. This indicates that the present homo-bimetallic complexes possess unsymmetrical biting sites (aminic and iminic) and the metal ions approach closely to these aza centers.

3.3. *Cyclic voltammetric studies*

The redox behaviors of $Co_2LCl_2(ClO_4)_2$, $Ni_2LCl_2(ClO_4)$, and $Cu_2LCl_2(ClO_4)_2$ were studied in the potential range +1.6 to −1.6 at three different scan rates (0.1, 0.2, 0.3 Vs^{-1}). The electrochemical data, magnitudes of reduction potential (E_p^c), oxidation

Table 4. Computed bond lengths and angles (A°) of the ligand and complexes.

	Ligand	**1**	**2**	**3**
C–N$_{ali.}$	1.377	1.377	1.377	1.377
C–N$_{aro}$	1.462	1.462	1.462	1.642
C=N	1.260	1.377	1.377	1.377
N–N	1.417	1.497	1.497	1.497
M–N	–	1.860	1.826	1.840
M–O	–	1.800	1.790	1.810
M–Cl	–	2.150	2.140	2.160
N–N=C	107.5	109.4	109.4	109.4
N–C=N	109.4	109.4	109.4	109.4
C–N–C	116.0	118.0	114.6	117.5
N–C–C	122.6	122.6	122.6	122.6
N=CC	117.3	117.3	117.3	117.3
N–M–N	–	119.5	119.9	90.0, 142.0
Cl–M–O	–	180.0	180.0	179.9

Table 5. Electrochemical data of 10^{-3} M solution of complexes recorded in DMSO at room temperature.

S. No.	Compounds	E_p^c (Volts)	$E_{1/2}^0$ (Volts)	E_p^a (Volts)
1	$Co_2LCl_2(ClO_4)_2$	-0.40_{irr} [a]		–
		-1.15^a	-1.075_{qr} [a]	-1.0^a
				$+0.2_{irr}$ [a]
2	$Ni_2LCl_2(ClO_4)_2$	-1.15_{xrr} [a]		
		-1.30^a	-1.17_{qr} [a]	-1.05^a
		-1.35^b	-1.20_{qr} [b]	-1.05^b
		-1.40^c	-1.22_{qr} [c]	-1.05^c
3	$Cu_2LCl_2(ClO_4)_2$	-0.282^b	-0.112_{qr} [b]	$+0.058^b$

[a]At 0.1 Vs^{-1} scan rate, [b]at 0.2 Vs^{-1} scan rate, [c]at 0.3 Vs^{-1} scan rate, irr = irreversible, qr = quasi-reversible.

potential (E_p^a) and the half wave potential ($E_{1/2}^\circ$) responsible for the formations of redox couples in solution have been summarized in table 5.

The cyclic voltamograms of **1** exhibit two cathodic peaks (figure 3a) while the reverse sweep contained only one anodic peak (table 5) with formation of a flattened quasi-reversible redox wave [37], consistent with a one step $2e^-$ reversible redox process $[Co^{II}LCo^{II}] \rightleftharpoons [Co^{I}LCo^{I}]$ to form the redox-couple at $E_{1/2}^\circ = -1.075$ V. A steep rise in current has been observed when the anodic potential approaches +0.3 V. This behaviour is probably due to a chemical disproportionation [38], i.e. $[Co^{I}LCo^{I}]$ $Co + [Co^{II}L]$.

The cyclic voltamograms for **2** (figure 3b) show a small negative shift in the positions of the cathodic peaks when the scan rate increased from 0.1–0.3 Vs^{-1}. The nature of the voltamograms at all three scan rates is nearly identical and is comparable to that observed for **1**. A one step, $1e^-$ reduction at each Ni(II) center produces the redox couple equilibrium $[Cu^{II}LCu^{II}] \rightleftharpoons [Cu^{I}LCu^{I}]$ for formation of the redox couple at $E_{1/2}^\circ \cong -1.20$ V (table 5). The redox-couple in **2** is generated at a higher cathodic potential compared to that for **1** (table 5), which may be ascribed to a disparity in the kinetic and or thermodynamic stabilities between +1 and +2 oxidation states of these $d^{6/7}$ and $d^{8/9}$ systems [39] (d^8 system is kinetically inert compared to d^6 system).

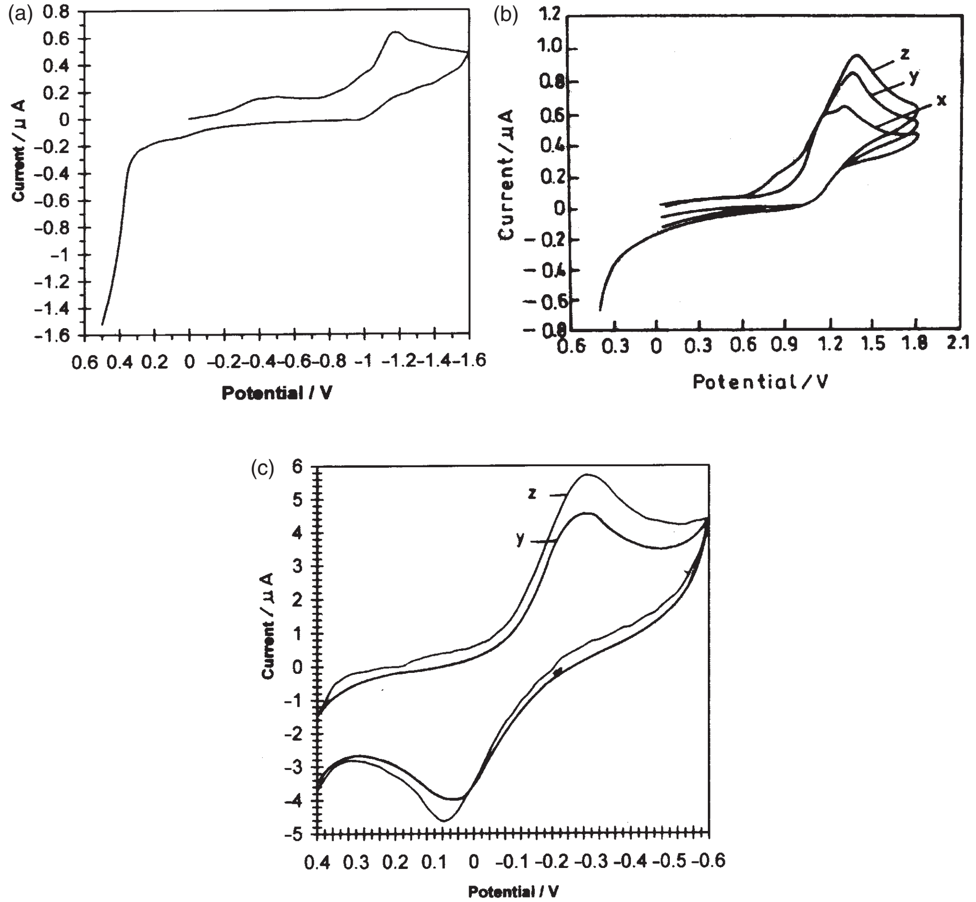

Figure 3. (a) Cyclic voltammogram of 10^{-3} M solution of **1** recorded in DMSO at room temperature using $[(n\text{-Bu})_4N]ClO_4$ supporting electrolyte at 0.1 Vs^{-1} scan rate. (b) Cyclic voltammogram of 10^{-3} M solution of **2** recorded in DMSO at room temperature using $[(n\text{-Bu})_4N]ClO_4$ supporting electrolyte at 0.1 Vs^{-1} (x), 0.2 Vs^{-1} (y) and 0.1 Vs^{-1} (z) scan rate. (c) Cyclic voltammogram of 10^{-3} M solution of **3** recorded in DMSO at room temperature using $[(n\text{-Bu})_4N]ClO_4$ supporting electrolyte at 0.2 Vs^{-1} (y) and 0.1 Vs^{-1} (z) scan rate.

The cyclic voltamograms for **3** recorded at 0.2 and 0.3 Vs^{-1} scan rates (figure 3c) exhibit a symmetrical voltamogram with a half wave potential, $E°_{1/2} = -0.11$ V (table 5). The electrochemical behavior of **3** is radically different from that reported [40] for the analogous homo–bimetallic Cu(II) complexes of acyclic polydentate chelating ligands. Complexes with acyclic ligands usually exhibit irreversible cathodic and anodic peaks consistent with the presence of a chemical disproportion process, resulting in deposition of metallic copper at electrode surfaces [40]. It is therefore reasonable to suggest that **3** undergoes a one step $1e^-$ redox process at each Cu(II) center of the homo–bimetallic complex $[Cu^{II}LCu^{II}]$ to generate a $[Cu^{I}LCu^{I}]$ species consistent with the reversible redox process $[Cu^{II}LCu^{II}] \rightleftharpoons [Cu^{I}LCu^{I}]$. The two redox species are considerably stabilized under electrochemical conditions by the present dinucleating unsymmetrical macrocyclic ligand. This reflects a non-rigid (or flexible) nature [3c, 31] of the macrocyclic cavity, which stabilizes lower (+1) as well as higher (+2) oxidation states of the metal ions.

3.4. *Evaluation of first ionic association constant, K_1 and free energy change (ΔG) from conductometric studies*

Thermodynamic ionic association constant as well as the corresponding free energy change (ΔG) of the metal encapsulated macrocyclic complexes **1**–**3** in DMSO has also been estimated by carrying out the conductometric studies at room temperature. Conductometric data were treated according to the modified Onsagar limiting equation employing Fuoss and Edelson method [41]. The Onsagar limiting equation is $\Lambda = \Lambda - \mathrm{S} \cdot \mathrm{C}_o^{1/2}$ (Λ is the equivalent conductance, $\mathrm{C_o}$ is appropriate concentration, Λ° is the limiting equivalent conductance and S represents the slope of the plot of Λ *vs.* $\mathrm{C}_o^{1/2}$). At low concentrations of the electrolyte, the Onsagar limiting law transforms to $\Lambda F = \Lambda^\circ - \mathrm{DK}_{1/}\Lambda^\circ$, where $\mathrm{D} = \mathrm{C_o} f_{2+} \Lambda F(\Lambda F - \Lambda^\circ/2)$ and $F = [(1 - \delta \mathrm{C}_o^{1/2})^{-1} + (\Lambda^\circ - \lambda_{'\circ-})/2\Lambda]/[1 + (\Lambda^\circ - \lambda'_{\circ-})\ 2\Lambda^\circ]$. Here K_1 is first ionic association constant and F is a function which corrects [3a] the conductance ratio, Λ/Λ°. The parameter δ is the ratio of the slope (S) and the limiting equivalent conductance (Λ°) of the complex cations and $\lambda'_{\circ-}$ is the anionic mobility (for $\mathrm{ClO_4^-}\,\lambda^\circ_- = 70.9\ \mathrm{ohm\,cm^2\,mol^{-1}}$).

The experimental equivalent conductivity data as well as the calculated magnitude of the relevant thermodynamic parameters are summarized in table 6. The slope of the plot of ΛF *versus* D has provided the magnitude of (K_1/Λ°), which ultimately gives the

Table 6. Magnitudes of experimental and calculated parameters from conductivity data of metal complexes in DMSO at room temperature.

Comp.	Concentration ($\mathrm{mol\,L^{-1}}$)	Λ (Ohm $\mathrm{cm^2\,mol^{-1}}$)	Λ° (Ohm $\mathrm{cm^2\,mol^{-1}}$)	F	D	K_1 ($\mathrm{L\,mol^{-1}}$)	$-\Delta G$ ($\mathrm{KJ\,mol^{-1}}$)
1	1×10^{-3}	62	125	1.0247	5.6870		
	7×10^{-4}	66		1.7619	3.3235		
	5×10^{-4}	81		1.5539	3.1592		
	3×10^{-4}	91		1.3819	1.9918		
	2.4×10^{-4}	98		1.3278	1.7908		
	1×10^{-4}	105		1.1908	0.7044		
	5×10^{-5}	108		1.1335	0.3406		
						16.66	6.97
2	1×10^{-3}	54	83	1.6986	3.3113		
	7×10^{-4}	55		1.5295	1.9052		
	5×10^{-4}	59		1.4139	1.3853		
	3×10^{-4}	65		1.2930	0.8953		
	2.4×10^{-4}	67		1.2604	0.7381		
	1×10^{-4}	77		1.1463	0.3719		
	5×10^{-5}	94		1.0878	0.2713		
						453	15.10
3	1×10^{-3}	54	74	1.5081	2.6012		
	7×10^{-4}	55		1.3925	1.6110		
	5×10^{-4}	57		1.3130	1.1220		
	3×10^{-4}	62		1.2344	0.7576		
	2.4×10^{-4}	65		1.2020	0.6541		
	1×10^{-4}	67		1.1195	0.2568		
	5×10^{-5}	74		1.0806	0.1545		
						434	15.04

magnitudes of the first ionic association constant (K_1). The corresponding free energy change ΔG has been obtained using the thermodynamic relationship $\Delta G = -RT \ln \mathrm{K}_1$. The magnitudes of first ionic-association constant (K_1) and the free energy change (ΔG) for complexes vary in the order $\mathrm{Ni}^{2+} \cong \mathrm{Cu}^{2+} > \mathrm{Co}^{2+}$. However, the magnitude of K_1 for the present homo–bimetallic complexes with [N_{10}] macrocycle is lower compared to that reported [42] for the corresponding complexes with [N_6] macrocycles. This reflects the existence of a strong ion-pair formation tendency for the present complexes in solution.

4. Conclusion

The macrocyclic ligand, 2,8,11,17-tetramethyl-3,5,7,12,14,16-hexaphenyl-[1,3,5,7,9,10,12,14,16,18]decaazaoctadeca-2,8,11,17-tetraene dihydroperchlorate ($\mathrm{L} \cdot 2\mathrm{HClO_4}$) is an example of an unsymmetrical dinucleating [N_{10}] macrocycle which encapsulates two metal ions via coordination from both aminic as well as iminic aza binding sites. The Co^{2+} and Ni^{2+} ions are five-coordinate, trigonal-bipyramidal while Cu^{2+} is six-coordinate. Bimetallic coordination by the macrocyclic ligand is retained even under FAB-Mass spectral conditions. The molecular model computations suggest that encapsulation of metal ions is effective to bring the chelating aza sites [N,N,N] or [N,N,N,N] in the basal plane of the macrocyclic cavities. The electro-chemical data are consistent with the flexible nature of the macrocyclic cavity.

Acknowledgements

The authors are thankful to Chairman, Department of Chemistry, Aligarh Muslim University, Aligarh, India, for providing necessary research facilities. Financial support from University Grant Commission, New Delhi, India, in the form of a Research Grant is gratefully acknowledged.

References

[1] Z. Hong, P. Zhen-He, P. Zia-Quan, L. Bo, H. Xue-Lei, L.Y. Qwing. *J. Coord. Chem.*, **58**, 443 (2005).

[2] (a) S. Brookers, P.D. Croucher. *J. Chem. Soc., Chem. Commun.*, 459 (1997); (b) S. Brooker, P.D. Croucher. *J. Chem. Soc., Chem. Commun.*, 2075 (1995); (c) S. Brookers, P.D. Croucher. *J. Chem. Soc., Dalton Trans.*, 1151 (1998).

[3] (a) Z.A. Siddiqi, M.M. Khan. *Synth. React. Inorg. Met.-Org. Chem.*, **34**, 897 (2004); (b) Z.A. Siddiqi, M. Khalid, M.M. Khan. *Polish J. Chem.*, **80**, 377 (2006); (c) Z.A. Siddiqi, Mohd. Khalid, S. Kumar. *Trans. Met. Chem.*, **32**, 913 (2007).

[4] H. Han, W.J. Raun, X.J. Zho, G.H. Hue, Z.A. Zhu. *Synth. React. Inorg. Met. Org. Chem.*, **33**, 1011 (2003).

[5] T. Klabunde, B. Krebs. *Struct. Bonding (Berlin)*, **89**, 177 (1997).

[6] H. Okawa, S. Kida, D.E. Fenton. *Inorg. Chem.*, **32**, 2949 (1993).

[7] E. Jabri, M.H. Lee, R.P. Hausinger, P.A. Karplus. *J. Mol. Biol.*, **227**, 934 (1992).

[8] E.I. Solomon, M.J. Baldwin, M.D. Lowery. *Lowery, Chem. Rev.*, **92**, 521 (1992).

[9] T.F. Pauwels, W. Lippens, G.G. Herman, A.M. Goeminne. *Polyhedron*, **17**, 1715 (1998).

[10] L. Bordignon, T. Marilde, B. Szpoganicz, M. Rizzoto, A.E. Martell, M.G. Basallote. *Inorg. Chim. Acta*, **254**, 345 (1997).

[11] P. Jurek, A.E. Martell. *Inorg. Chem. Acta*, **287**, 47 (1999).

[12] P. Zanello. *Coord. Chem. Rev.*, **77**, 265 (1987).

[13] R.E. Stenkamp, L.C. Sieker, L.H. Jensen, J.D. McCallum, J. Sanders-Loehr. *J. Proc. Natl. Acad. Sci., USA*, **82**, 713 (1985).

[14] B.G. Fox, M.P. Hendrich, K.K. Surerus, K.K. Andersson, W.A. Froland, J.D. Lipscomb, E. Munck. *J. Am. Chem. Soc.*, **115**, 3688 (1993).

[15] A.C. Rosenzweig, C.A. Frederick, S.J. Lippard, P. Nerdlund. *Nature*, **366**, 537 (1993).

[16] (a) P.A. Vigato, S. Tumburini, D.E. Fenton. *Coord. Chem. Rev.*, **106**, 25 (1990); (b) V. Alexander. *Chem. Rev.*, **95**, 273 (1995).

[17] M. Marappan, V. Narayanan, M. Kandaswamy. *J. Chem. Soc., Dalton Trans.*, **20**, 3405 (1998).

[18] F.A. Cotton, O.D. Faut, D.M.L. Goodgame, R.H. Holm. *J. Chem. Soc.*, **83**, 1780 (1961).

[19] K. Motrado, H. Sakiyama, N. Matsumoto, H. Okawa, D. Fenton. *J. Chem. Soc., Dalton Trans.*, 3419 (1995).

[20] J.L. Sesser, T.D. Mody, V. Lynch. *Inorg. Chem.*, **31**, 529 (1992).

[21] K. Nakamoto. *Infrared and Raman Spectra of Inorganic and Coordiantion Compounds*, 4th Edn, A. Wiley-Interscience Publication, (1986).

[22] M.R. Rosenthal. *J. Chem. Soc.*, **50**, 331 (1973).

[23] W.J. Geary. *Coord. Chem. Rev.*, **7**, 81 (1971).

[24] T. Kurisaki, T. Yamaguchi, M. Fujiwala, R. Kiraly, H. Wakita. *J. Chem. Soc., Dalton Trans.*, 3727 (1996) and references cited therein.

[25] J. Lewis, R.G. Wilkins. *Modern Coordination Chemistry*, Interscience Publisher, New York (1960).

[26] C.W. Yan, T.L. Yan, Y.Z. Chum, S.G. Hua. *Synth. React. Met. Org. Chem.*, **34**, 929 (2004).

[27] (a) Y.T. Li, C.W. Yan, S.H. Maio, D.Z. Lio. *Polyhedron*, **15**, 2491 (1998); (b) S.L. Lambert, C.L. Sapiro, R.R. Gange, D.N. Hendrickson. *Inorg. Chem.*, **21**, 68 (1982).

[28] K. Hayland, I. Riosin, H. Bamound, C. Auckkair. *Anal. Biochem.*, **135**, 80 (1983).

[29] S.K. Mandal, K. Nag. *J. Chem. Soc., Dalton Trans.*, 2141 (1984).

[30] A.B.P. Lever. *Inorganic Electronic Spectroscopy*, 2nd Edn, Elsevier, Amsterdam (1984).

[31] Z.A. Siddiqi, V.J. Jacob. *Polyhedron*, **13**, 799 (1994).

[32] G. Dyer, D.W. Meek. *J. Am. Chem. Soc.*, **89**, 3983 (1967).

[33] B.N. Figgis, R.S. Nyhdm. *J. Chem. Soc.*, 12 (1954).

[34] J.J.P. Steward. *J. Comp. Chem.*, **10**, 221 (1989).

[35] D. Hinks, J. Lye, H.S. Freeman. *Computer Aided Dyestuff Design*, pp. 74–85, Book of papers-AATCC, International Conference and Exhibition, Atlanta, Georgia (1995).

[36] P.V. Bernhardt, G.A. Lawrence. *Coord. Chem. Rev.*, **104**, 297 (1990).

[37] M. Adachi, K.M. Kita, K. Fujita, N. Kurachi, S. Ohba, D. Jin. *Bull. Chem. Soc. Jap.*, **65**, 2037 (1992).

[38] M. Bonamico, V. Fares, A. Flamini, N. Poli. *J. Chem. Soc., Dalton Trans.*, 3273 (1992).

[39] F.A. Cotton, G. Wilkinson. *Advanced Inorganic Chemistry*, p. 652, Wiley Eastern Ltd., N. Delhi (1976).

[40] C. Dendrinou-Samara, P.D. Janakoudakis, D.P. Kessissaglou, G.E. Manoyussakis, D. Mentzapfos, A. Terzis. *J. Chem. Soc., Dalton Trans.*, 3259 (1992).

[41] R.M. Fuoss, D. Edelson. *J. Am. Chem. Soc.*, **73**, 269 (1951).

[42] J. Liu, Y. Masuda, E. Sekido. *Bull. Chem. Soc. Jpn.*, **63**, 2516 (1990).